



# Progression from remodeling to hibernation of ribosomes in zinc-starved mycobacteria

Yunlong Li<sup>a</sup>, Jamie H. Corro<sup>a,b</sup>, Christopher D. Palmer<sup>c,d</sup>, and Anil K. Ojha<sup>a,b,1</sup>

<sup>a</sup>Division of Genetics, Wadsworth Center, New York State Department of Health, Albany, NY 12208; <sup>b</sup>Department of Biomedical Sciences, School of Public Health, University at Albany, Albany, NY 12222; <sup>c</sup>Laboratory of Inorganic and Nuclear Chemistry, Wadsworth Center, New York State Department of Health, Albany, NY 12202; and <sup>d</sup>Department of Environmental Health Sciences, University at Albany, Albany, NY 12222

Edited by William R. Jacobs Jr., Albert Einstein College of Medicine, Bronx, NY, and approved July 6, 2020 (received for review June 30, 2020)

Zinc starvation in mycobacteria leads to remodeling of ribosomes, in which multiple ribosomal (r-) proteins containing the zinc-binding CXXC motif are replaced by their motif-free paralogues, collectively called C- r-proteins. We previously reported that the 70S C- ribosome is exclusively targeted for hibernation by mycobacterial-specific protein Y (Mpy), which binds to the decoding center and stabilizes the ribosome in an inactive and drug-resistant state. In this study, we delineate the conditions for ribosome remodeling and hibernation and provide further insight into how zinc depletion induces Mpy recruitment to C- ribosomes. Specifically, we show that ribosome hibernation in a batch culture is induced at an approximately two-fold lower cellular zinc concentration than remodeling. We further identify a growth phase in which the C- ribosome remains active, while its hibernation is inhibited by the caseinolytic protease (Clp) system in a zinc-dependent manner. The Clp protease system destabilizes a zinc-bound form of Mpy recruitment factor (Mrf), which is stabilized upon further depletion of zinc, presumably in a zinc-free form. Stabilized Mrf binds to the 30S subunit and recruits Mpy to the ribosome. Replenishment of zinc to cells harboring hibernating ribosomes restores Mrf instability and dissociates Mpy from the ribosome. Finally, we demonstrate zinc-responsive binding of Mpy to ribosomes in *Mycobacterium tuberculosis* (Mtb) and show Mpy-dependent antibiotic tolerance of Mtb in mouse lungs. Together, we propose that ribosome hibernation is a specific and conserved response to zinc depletion in both environmental and pathogenic mycobacteria.

persistence | tuberculosis | drug tolerance | ribosome hibernation | Clp protease

**T**uberculosis (TB), caused by *Mycobacterium tuberculosis* (Mtb), kills more people worldwide every year than any other bacterial pathogen (1). Among the unmet challenges toward an effective control of TB, is a shorter treatment regimen comprising drugs that can target a small subpopulation of persistent bacilli exhibiting phenotypic tolerance to antibiotics. While factors inducing the development of Mtb persisters in hosts remain unclear, it is hypothesized that these bacilli represent a nonreplicating physiological state characterized by slow metabolism (2).

In many bacterial species, stresses leading to growth stasis induce hibernation of ribosomes, either as monosomes (70S) or disomes (100S), by specialized proteins (protein Y for 70S or Hpf for 100S) that bind near the decoding center on the 30S subunit at the intersubunit interface (3–15). Although the functional consequences of ribosome hibernation remain to be fully understood, the process appears to slow down the degradation of ribosomes in growth-arrested cells, while promoting cell survival and tolerance to antibiotics (12, 16–20). Given the widespread phenomenon of ribosome hibernation in bacteria (21), molecular mechanisms underlying the formation of a hibernating ribosome complex, and its reactivation during resuscitation of cells, are likely to offer new therapeutic strategies against growth-arrested bacteria. Factors underlying the regulation of ribosome hibernation have largely been described in the context of the formation of

100S disomes (17, 22–25), whereas those regulating the hibernation of 70S monosomes remain unclear.

We previously discovered that hibernation of 70S ribosomes in *Mycobacterium smegmatis* occurs specifically under zinc starvation (12). Zinc starvation also induces remodeling of ribosomes, in which ribosomal (r-) proteins with the zinc-binding CXXC motif (called C+ r-proteins) are replaced by their C- paralogues lacking the motif (12, 26, 27). Genes encoding the five C- r-proteins are organized in an operonic structure, which is transcriptionally controlled by a zinc uptake repressor, Zur (*SI Appendix, Fig. S1*) (12). Transcriptional derepression of c- operon under zinc-depleted conditions leads to assembly of C- ribosomes (12). An apparent purpose of C+ to C- replacements is to restore zinc homeostasis, presumably by reducing the zinc demand and temporarily increasing the supply by releasing zinc atoms from preexisting C+ ribosomes. Consistently, mycobacterial mutants of c- operon are hypersensitive to zinc starvation (12, 28). During a structure–function analysis of C- ribosomes, we observed that these ribosomes are the specific target of mycobacterial-specific protein Y (Mpy) that inactivates and stabilizes 70S monosomes in a conformation with reduced sensitivity to kanamycin and streptomycin (Str) (12). While Mpy expression is constitutive, its binding to the 70S ribosome is induced by an Mpy recruitment factor (Mrf), which is also encoded within c- operon (12). Interestingly, an engineered constitutive

## Significance

**We previously reported that hibernation of 70S ribosomes in mycobacteria is induced as a response to zinc starvation. Because zinc limitation also induces ribosome remodeling, our findings raise questions about the conditions for ribosome remodeling and hibernation. Here, we show that the two processes are induced at different concentrations of zinc and that the caseinolytic protease system plays a crucial role in zinc-dependent inhibition of hibernation during remodeling. The findings offer insights into the molecular pathway underlying the transition from remodeling of ribosomes to hibernation in response to progressive zinc depletion in mycobacteria. This study is also a demonstration of reactivation of hibernating ribosomes by zinc. Finally, this study correlates ribosome hibernation with streptomycin tolerance in *Mycobacterium tuberculosis* during infection.**

Author contributions: Y.L., J.H.C., and A.K.O. designed research; Y.L., J.H.C., and A.K.O. performed research; Y.L., J.H.C., C.D.P., and A.K.O. contributed new reagents/analytic tools; Y.L., J.H.C., and A.K.O. analyzed data; and Y.L., J.H.C., C.D.P., and A.K.O. wrote the paper.

The authors declare no competing interest.

This article is a PNAS Direct Submission.

This open access article is distributed under [Creative Commons Attribution-NonCommercial-NoDerivatives License 4.0 \(CC BY-NC-ND\)](https://creativecommons.org/licenses/by-nc-nd/4.0/).

<sup>1</sup>To whom correspondence may be addressed. Email: anil.ojha@health.ny.gov.

This article contains supporting information online at <https://www.pnas.org/lookup/suppl/doi:10.1073/pnas.2013409117/-DCSupplemental>.

First published July 28, 2020.

expression of *c*- operon is sufficient for the assembly of C- ribosomes in high-zinc growth conditions, but not for inducing Mpy recruitment, for which zinc depletion is necessary (12). We therefore inferred that ribosome remodeling and hibernation require distinct conditions, and additional unidentified regulators are involved in creating this distinction. Here, we resolve ribosome remodeling from hibernation and demonstrate that the remodeled ribosome remains active in a growth phase, during

which hibernation of the remodeled ribosome is inhibited by the caseinolytic protease (Clp) system. We subsequently elucidate the relationship between zinc and Clp-dependent Mrf instability and identify the condition under which Mrf is stabilized to induce ribosome hibernation. By demonstrating the reactivation of hibernating ribosomes by zinc replenishment, we establish an unambiguous relationship between zinc depletion and ribosome hibernation. Finally, we provide data highlighting the importance

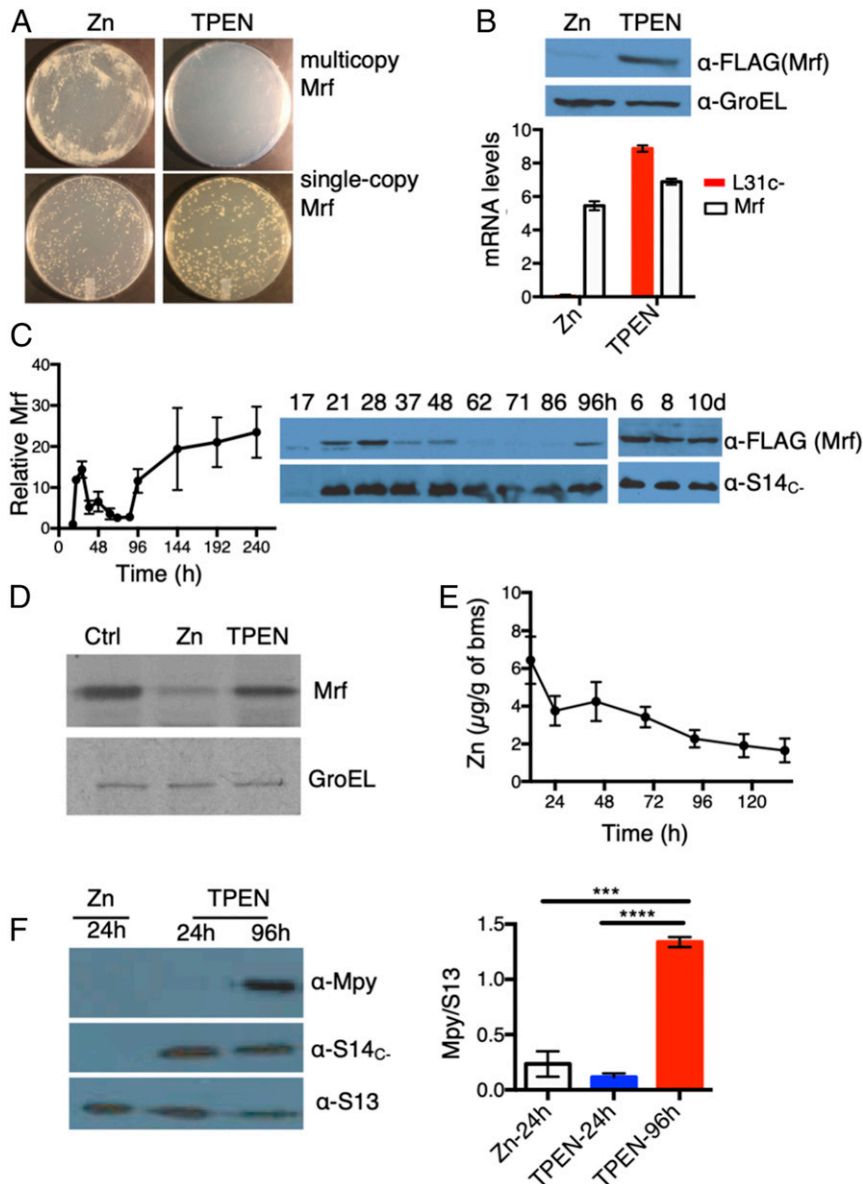


**Fig. 1.** Remodeling and hibernation of ribosomes are induced at different zinc levels. (A) Plating efficiencies of strains constitutively expressing single-copy (YL7) or multicopy Mrf (YL8) on high- or low-zinc Sauton's agar plates imaged by a digital single-lens reflex camera at 1× magnification. (B) Zinc-dependent loss of Mrf stability in the YL7 strain. The plot shows mRNA levels of Mrf and L31c<sub>-</sub> (normalized to SigA) in high- and low-zinc culture after 96 h of growth. The immunoblot above shows corresponding levels of Mrf protein in the samples used for mRNA quantitation. (C) Levels of Mrf protein in the YL2 strain (expressing Mrf from the native promoter on an integrative plasmid) at indicated time points of growth in low-zinc Sauton's medium (h and d denote hours and days postinoculation, respectively). S14c<sub>-</sub> was probed to monitor the transcriptional induction of *c*- operon. (D) Level of <sup>35</sup>S-labeled Mrf immunoprecipitated from 96-h low-zinc cultures of the YL7 strain (Ctrl) after a 60-min exposure to label-free high-zinc (Zn) or zinc-depleted (TPEN) Sauton's medium. Mrf was labeled by addition of 10 μCi/mL of [<sup>35</sup>S]methionine to a 96-h low-zinc culture of YL7 for 2 h; then labeled cells were washed and exposed to label-free medium for 60 min prior to immunoprecipitation of Mrf. GroEL was immunoprecipitated from the same lysates as control. (E) Zinc content in biomass (bms) collected at indicated time points of growth of a batch culture of *M. smegmatis* in low-zinc Sauton's medium. Each data point represents an average measurements of three biologically independent cultures. (F) Mpy levels in ribosomes purified at two time points representing transcription (24 h) and accumulation (96 h) of Mrf. Ribosomes from a 24-h-old high-zinc culture served as the negative control. The plot shows average Mpy levels (normalized to S13) in each condition. Data in B, C, E, and F represent mean ± SD from three biologically independent replicates. \*\*\**P* < 0.001 and \*\*\*\**P* < 0.0001 (*t* test).

of zinc-responsive binding of Mpy to ribosomes in drug tolerance of Mtb during infection.

## Results

### Posttranslational Degradation of Mrf during Ribosome Remodeling.

Previously, we showed that Mpy recruitment to C- ribosomes was reduced in a strain carrying an in-frame deletion in *mrf* (12). The mutant phenotype was complemented by C-terminally FLAG-tagged Mrf in strain YL2 (*SI Appendix, Fig. S1*). We thus chose Mrf-FLAG (henceforth called Mrf) as a probe to address why a constitutive expression of Mrf is not sufficient to

induce Mpy recruitment in high-zinc medium (12). We fortuitously observed that constitutive expression of Mrf from a multicopy episomal plasmid in a  $\Delta mrf$  background (strain YL8) was toxic in low-zinc medium containing 1  $\mu$ M TPEN (*N,N,N,N*-tetrakis(2-pyridinylmethyl)-1,2-ethanediamine), but not in high-zinc medium containing 1 mM ZnSO<sub>4</sub>, although constitutive Mrf expression from a chromosomally integrated plasmid in a  $\Delta mrf$  background (strain YL7) was tolerated under both conditions (Fig. 1A). The zinc-dependent toxicity of multicopy Mrf was also recapitulated by its constitutive expression from the native promoter in a  $\Delta zur$  mutant (*SI Appendix, Fig. S2A*). The multicopy

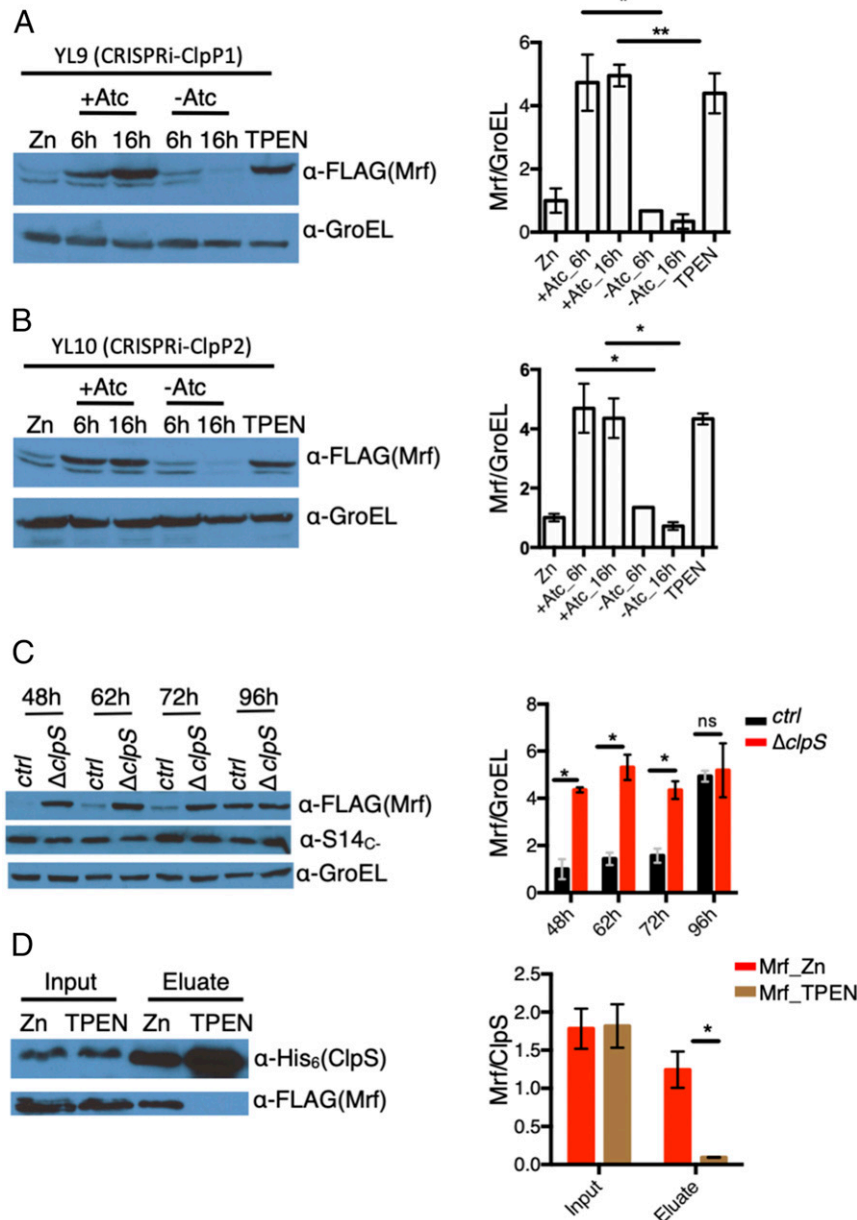


**Fig. 2.** Clp-dependent loss of Mrf stability in high-zinc medium. (A and B) Accumulation of Mrf upon depletion of either ClpP1 in strain YL9 (A) or ClpP2 protease in strain YL10 (B). Cells were cultured in high-zinc Sauton's medium and guide RNA corresponding to ClpP1 (A) or ClpP2 (B) was induced with Atc for 6 or 16 h prior to Mrf analysis. Uninduced cultures at corresponding time points and high- or low-zinc cultures of each strain were controls. The minor band below Mrf is unrelated to the FLAG signal that also appears in lysates of the parent strains. (C) Analysis of Mrf levels in YL2 (*ctrl*) strain or its isogenic  $\Delta clpS$  mutant (YL15) at indicated time points of growth in low-zinc Sauton's medium. (D) Coelution of Mrf from high- or low-zinc cultures of YL16—a derivative of YL9 that expressed ClpS<sub>6xHis</sub>—on Ni-NTA matrix. Mrf from high-zinc culture was analyzed upon depletion of ClpP1. The plots to the right of each immunoblot show the average normalized Mrf signal from three biologically independent experiments. \**P* < 0.05 and \*\**P* < 0.01 (*t* test).

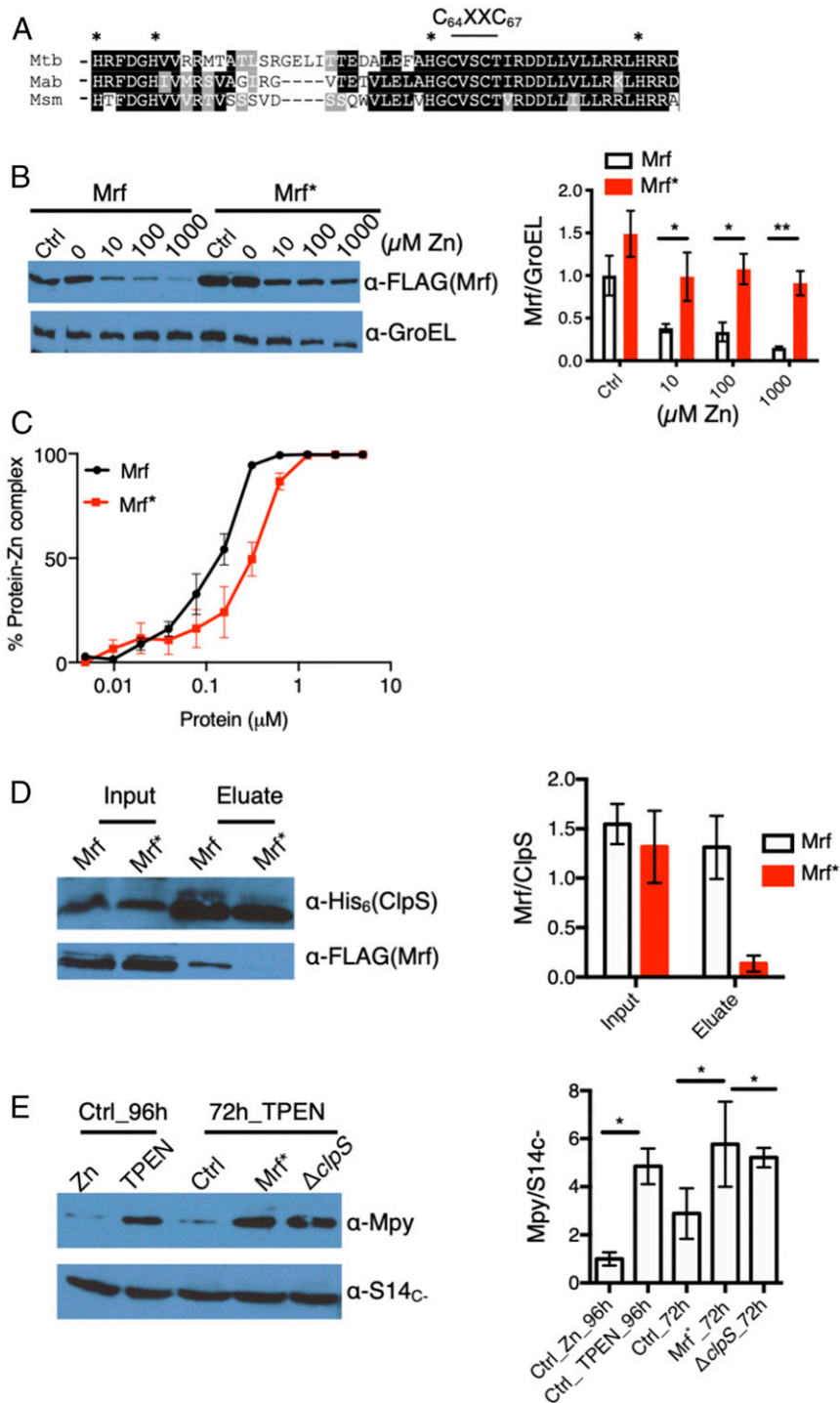


**Fig. 3.** Affinity for zinc in Mrf determines its interaction with ClpS. (A) The N-terminal regions of Mrf from three mycobacterial species showing putative Zn-binding CXXC and flanking His residues. (B) Stability of Mrf in strain YL20 and Mrf\* (carrying the Ala substitutions for H36, H41, H62, C64, C67, and H81) in strain YL21 analyzed from 96-h cultures grown in Sauton's medium containing indicated concentrations of supplemental ZnSO<sub>4</sub>. A culture in low-zinc Sauton's medium containing 1 μM TPEN was used as control (Ctrl). GroEL was probed as normalizing control. (C) Titration of free zinc in a solution containing 5 μM ZnSO<sub>4</sub> and indicated concentrations of Mrf or Mrf\*. Each point represents the average of three independent experiments. The protein-zinc mixture was equilibrated at room temperature for 30 min prior to adding 10 μM FluoZin-3. The y axis showing the percentage of protein-zinc complex was derived from the fraction of fluorescence signal from free zinc in the reaction to that from total zinc in a protein-free control. (D) Coelution of either Mrf or Mrf\* with ClpS<sub>6XHis</sub> from lysates of YL16 and YL17, respectively, on Ni-NTA matrix. Cells were cultured in high-zinc medium, and ClpP1 was depleted with Atc for 16 h before purification ClpS<sub>6XHis</sub> on Ni-NTA matrix. (E) Levels of Mpy associated with purified ribosomes from YL2 (ctrl), YL15 (ΔclpS), and YL28 (Mrf\*) strains at the 72-h time point of growth in low-zinc Sauton's medium. Ribosomes from YL2 cells cultured either in high- or low-zinc medium for 96 h were used as controls. S14c<sub>-</sub> was probed as the loading control. Plots on the right of B, D, and E show the normalized average density of Mrf or Mpy from two (for D) or three (B and E) biologically independent experiments. \*P < 0.05 and \*\*P < 0.01 (t test).

expression produced greater Mrf levels than single-copy expression (*SI Appendix, Fig. S2B*), suggesting a correlation between protein abundance and toxicity. Deletion of *mpy* failed to rescue the toxic effect of Mrf overexpression (*SI Appendix, Fig. S2C*), ruling out the possibility that premature hibernation of ribosomes by Mpy was a cause for toxicity. The *in vitro* translation activity of ribosomes purified from a low-zinc culture of the  $\Delta mpy/\Delta mrf$  strain was significantly more than that from  $\Delta mpy$  (*SI Appendix, Fig. S2D*), suggesting that translation inhibition, presumably by Mpy-independent binding of Mrf to ribosomes, is the likely cause of toxicity.

Because zinc supplementation could rescue the dose-dependent toxicity of Mrf (Fig. 1A), we hypothesized that zinc could be regulating Mrf stability at the posttranscriptional level. Regardless of constitutive messenger RNA (mRNA) levels of Mrf in both high- and low-zinc cultures of YL7 strain, Mrf protein was detected only under low-zinc conditions (Fig. 1B and *SI Appendix, Fig. S2E*). To delineate the precise timing of the expression of *c-* operon and Mrf stabilization, we examined the accumulation of Mrf protein relative to a C- ribosomal protein (S14<sub>C-</sub>) at regular intervals during growth of the YL2 strain in a low-zinc culture. The levels of S14<sub>C-</sub> increased sharply by 21 h post inoculation, likely from progressive depletion of contaminating zinc in the batch culture, and remained largely unchanged during further growth (Fig. 1C). The Mrf level increased transiently between 21 and 28 h and then progressively diminished before reappearing at ~96 h, after which it remained steady (Fig. 1C). Interestingly, the transient accumulation of Mrf was responsive to Zur; an isogenic  $\Delta zur$  mutant did not accumulate Mrf until ~96 h of growth (*SI Appendix, Fig. S2F*). Thus, it appears that transient (~17 to 28 h) and permanent (after 96 h) accumulation of Mrf are mechanistically distinct outcomes. Nonetheless, zinc as a necessary and specific signal for post-translational regulation of Mrf is further supported by a substantial loss of Mrf stability upon addition of 1  $\mu$ M ZnSO<sub>4</sub>, but no other common divalent metal ions, to 96-h-old low-zinc cells (*SI Appendix, Fig. S3 A–C*). To test if zinc-responsive Mrf accumulation is a consequence of its increased synthesis or decreased turnover, we pulse-labeled Mrf with <sup>35</sup>S-Met in a 96-h low-zinc culture of the YL7 strain and monitored the labeled protein after 60 min of incubation in label-free high- or low-zinc medium. While no apparent change in <sup>35</sup>S-Mrf was observed in low-zinc medium, the labeled protein was substantially decreased in high-zinc medium (Fig. 1D), indicating that preexisting Mrf is degraded in cells upon zinc exposure.

The data so far support a hypothesis that ribosome remodeling occurs at a zinc concentration that is sufficient to destabilize Mrf, thereby preventing Mpy recruitment to the ribosome until further zinc depletion stabilizes Mrf. To test, we determined the cellular zinc content and the abundance of Mpy-bound ribosomes in cells at the 24- and 96-h stages—the time points associated with ribosome remodeling and Mrf stabilization (Fig. 1C). Using Inductively Coupled Plasma Mass Spectrometry (ICP-MS), we determined zinc concentrations in aliquots of cells taken out at regular intervals from a low-zinc batch culture. Zinc content in cells at the 96-h stage was approximately two-fold lower than at the 24-h stage (Fig. 1E). Moreover, Mpy association with ribosomes was induced at 96-h, but not at the 24-h stage (Fig. 1F). Furthermore, cellular growth and global protein synthesis remained active at the 24-h stage, but reached stasis by the 96-h stage (*SI Appendix, Fig. S4 A and B*), indicating that ribosome remodeling is induced at a growth-permissive zinc concentration, whereas Mrf stabilization (and therefore ribosome hibernation) is induced under the zinc-depleted stationary phase.

#### Zinc-Dependent Mrf Degradation Requires the Clp Protease System.

To identify the protease responsible for zinc-dependent Mrf degradation, we used a strain that constitutively expressed Mrf

from an integrative plasmid and screened for Mrf stabilizing mutants in high-zinc medium. Deletions of genes encoding nonessential putative zinc metalloproteases or the proteasome subunits failed to stabilize Mrf in high-zinc medium. However, conditional depletion of either ClpP1 (YL9) or ClpP2 (YL10) using a CRISPRi system led to stabilization of Mrf under high-zinc conditions (Fig. 2A and B and *SI Appendix, Fig. S5 A–D*). Mycobacterial ClpP1P2 subunits are known to form a barrel-shaped hetero-tetradecameric peptidase complex (29), representing AAA+ family proteolytic machines that partner with an ATPase (ClpA/ClpC or ClpX) and an adaptor protein (SspB or ClpS) to degrade a broad range of target proteins containing specific sequence determinants, called degrons (30–36). Depletion of ClpX did not impact Mrf degradation, suggesting that ClpC1 (MSMEG\_6091) possibly serves as the ATPase in the process; mycobacteria do not encode a ClpA homolog. However, attempts to test the role of ClpC1 by CRISPRi were not successful due to partial depletion of corresponding transcripts. Because mycobacterial ClpC1 appears to interact with ClpS (37), we probed the role of ClpS in Mrf degradation. An isogenic  $\Delta clpS$  deletion (YL15) accumulated significantly more Mrf than the parent strain (YL2) at an early growth stage (Fig. 2C). Early stabilization of Mrf in a *clpS* mutant suggests that physiological interaction between Mrf and ClpS occurs at a zinc concentration below the level necessary for derepression of *c-* operon.

Because ClpS plays a crucial role in target recognition by the Clp protease system (30–36), we hypothesized that Mrf interacts with ClpS in a zinc-dependent manner. A strain (YL16) coexpressing Mrf and ClpS<sub>6xHis</sub>, while carrying the Atc-inducible CRISPRi system for ClpP1, was cultured in high- or low-zinc medium for 96 h, and ClpS-Mrf interaction was evaluated. To allow detectable Mrf accumulation in high-zinc medium, ClpP1 was depleted by inducing the CRISPRi system. ClpS interaction with Mrf in the YL16 strain was detectable only in cells from high-zinc medium (Fig. 2D).

**Affinity for Zinc in Mrf Determines Its Interaction with ClpS.** The canonical degrons for ClpS are generated upon posttranslational changes in the N-terminal sequences of target proteins (33, 36). The N-terminal sequence of Mrf, however, remained unchanged in high- and low-zinc medium (*SI Appendix, Fig. S6 A–D*), indicating that zinc-dependent degron formation in Mrf likely follows a noncanonical pathway, such as those described in *Salmonella enterica* (36). Because Mrf has the signature zinc-binding C<sub>64</sub>XXC<sub>67</sub> motif, which is flanked by four His (H<sub>36,41,62,81</sub>) (Fig. 3A), we hypothesized that Mrf binds to zinc, thereby generating the degron recognizable by ClpS. The zinc-binding property of Mrf was confirmed by ICP-MS, estimating up to three zinc atoms per protomer (*SI Appendix, Fig. S7A*). Furthermore, Ala substitutions of the two Cys in the C<sub>64</sub>XXC<sub>67</sub> motif, combined with the four His (H<sub>36,41,62,81</sub>), stabilized the resulting protein (called Mrf\*) in cells cultured in the presence of up to 1 mM ZnSO<sub>4</sub> (Fig. 3B). To directly correlate Mrf stability with its ability to bind zinc, we compared the zinc affinity of purified Mrf and Mrf\* using a zinc indicator, FluoZin-3 (*SI Appendix, Fig. S7B*). We titrated free zinc upon serially increasing the concentration of metal-stripped protein to a buffer containing 5  $\mu$ M ZnSO<sub>4</sub>. The assay reported approximately two-fold lower zinc affinity in Mrf\* relative to Mrf (Fig. 3C). The residual zinc affinity in the mutant suggests that there are additional zinc-coordinating amino acids in Mrf. Nonetheless, the correlation between loss of zinc affinity and stability of Mrf\* predicted a reduced Mrf\*-ClpS interaction in a high-zinc culture, which was verified by the data in Fig. 3D.

We further exploited the two Mrf-stabilizing mutants,  $\Delta clpS$  and Mrf\*, to test whether ectopic Mrf can induce Mpy recruitment to the C- ribosome under the physiological condition when the C- ribosome is active; for example, a 72-h stage of growth

(Fig. 2C). Mpy levels in the ribosomes purified from a 72-h culture of either the  $\Delta clpS$  strain (YL15) or a strain expressing Mrf\* (YL28) were significantly higher than a 72-h culture of the control strain (YL2), but similar to a 96-h YL2 culture (Fig. 3E).

**Direct Role of Mrf in Mpy Recruitment to C- Ribosomes.** The correlation between Mrf stability and ribosome hibernation raises the question as to how Mrf facilitates the formation of an Mpy-ribosome complex. Because Mpy contact points are predominantly on the 30S subunit (12), we hypothesized that Mrf binds to the 30S subunit to promote Mpy binding. We compared the relative abundance of Mpy and Mrf in ribosomes isolated from 96-h-old low-zinc cultures of strain YL18. Mpy was predominantly associated with the 70S ribosome, while the majority of Mrf was detected in the 30S fractions (Fig. 4A and *SI Appendix*,

Fig. S8A). A relatively small amount of Mrf was associated with the 70S ribosome (Fig. 4A), suggesting that a subsequent association of the Mrf-30S complex with either 50S or Mpy destabilizes Mrf. Binding of Mrf to the 30S subunit remained unchanged in a  $\Delta mpy$  strain (*SI Appendix*, Fig. S8B), indicating an Mpy-independent interaction of Mrf with ribosomes. To further assess the effect of Mrf on Mpy recruitment, we analyzed the formation of Mpy-70S complex upon addition of purified recombinant Mpy (rMpy) to C- ribosomes, which were isolated from low-zinc cultures of either  $\Delta mpy$  or  $\Delta mpy/\Delta mrf$  strains. Crude ribosomes mixed with rMpy for 1 h were resolved on a 5-mL linear 5 to 30% sucrose density gradient, and the 70S complex was analyzed with anti-Mpy antibody. Mpy association with the 70S ribosome isolated from a  $\Delta mpy$  strain was significantly more than that from the  $\Delta mpy/\Delta mrf$  double mutant

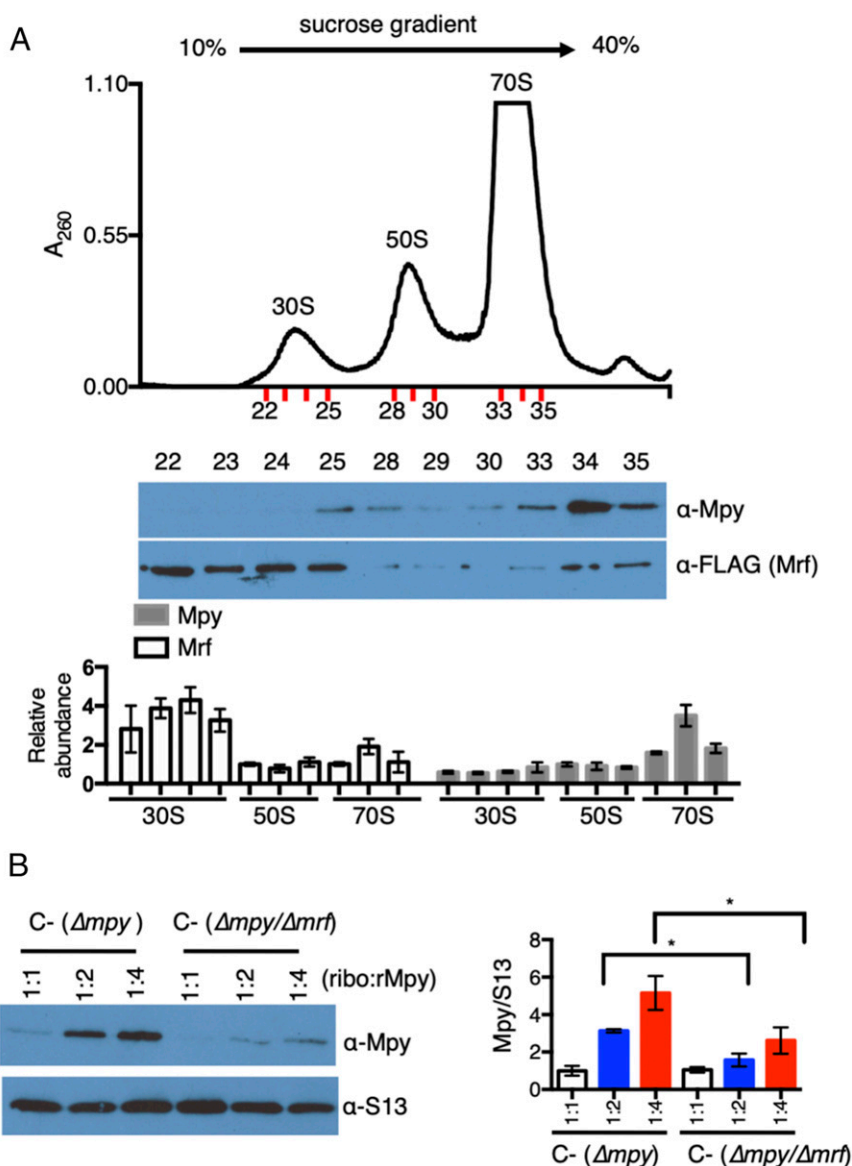


**Fig. 4.** Mrf promotes Mpy recruitment by modulating the ribosome. (A) Levels of Mrf and Mpy in 30S, 50S, and 70S ribosomes. Crude ribosomes from low-zinc cultures of the YL18 strain were resolved on a 12-mL sucrose density gradient (10 to 40%), and the fractions corresponding to the 30S, 50S, and 70S particles (indicated in red) were probed for Mrf and Mpy. The plot shows the average intensity of Mrf and Mpy signals in the 30S and 70S fractions, relative to the 50S fractions, from two biologically independent experiments. (B) *In vitro* association of recombinant Mpy (rMpy) to C- ribosomes purified from low-zinc cultures of either YL3 ( $\Delta mpy$ ) or YL4 ( $\Delta mpy/\Delta mrf$ ). Ribosomes purified on a sucrose cushion were mixed with rMpy at the indicated molar ratio for 60 min and then resolved on a 5-mL 5 to 30% sucrose density gradient. Fractions with 70S ribosomes were pooled and probed with anti-Mpy and anti-S13 (control) antibodies. The plot shows average rMpy signal in the indicated reactions from three biologically independent experiments. \* $P < 0.05$ .

(Fig. 4B), offering a biochemical evidence for a direct role of Mrf in Mpy recruitment, perhaps by modifying the ribosome. Similar results were obtained when rMPY association in mixtures containing the 50S subunit and either purified Mrf-30S from  $\Delta mpy$  or 30S from  $\Delta mpy/\Delta mrf$  strains were compared (SI Appendix, Fig. S9). The joining of the 50S subunit to a Mrf-30S complex also appears to be Mpy independent (SI Appendix, Fig. S9). Taken together, Mrf binding to the 30S subunit appears to be a crucial step in ribosome hibernation, upstream from Mpy recruitment and joining of the 50S subunit.

#### Reactivation of Hibernating C– Ribosomes upon Zinc Replenishment.

Degradation of preexisting Mrf upon zinc replenishment (Fig. 1D) raises the important question as to whether Mpy is also dissociated from the ribosome to facilitate its reactivation during growth regeneration. A 96-h low-zinc culture of YL2 was first conditioned in phosphate-buffered saline (PBS) with TPEN to minimize new synthesis of ribosomes and then exposed to PBS with 1 mM ZnSO<sub>4</sub> for 1 h. Incubation of cells in PBS with zinc resulted in both Mrf degradation (Fig. 5A) and dissociation of Mpy from the ribosome (Fig. 5B). The S14<sub>C–</sub> levels were unchanged (Fig. 5B), indicating that Mpy-free ribosomes remained C–, perhaps until fully turned over by further growth in zinc-rich medium. Ribosomes purified from cells upon zinc replenishment, following Mpy dissociation, exhibited increased translational activity in vitro compared to those from zinc-depleted cells harboring hibernating ribosomes (Fig. 5C). To correlate Mrf degradation with Mpy dissociation from the ribosome, we

compared the abundance of Mpy-bound ribosomes between cells expressing either Mrf (YL2) or Mrf\* (YL28) after reintroduction of zinc. Following treatments with up to 10 μM ZnSO<sub>4</sub>, Mpy dissociation was considerably reduced in YL28 compared to YL2 strain (Fig. 5D). Thus, dissociation of Mpy from the ribosome is dependent on degradation of Mrf, implying a role of Mrf in maintenance of the Mpy-bound ribosome. A tight correlation between Mrf degradation and Mpy dissociation further suggests that Mrf is probably an integral component of the hibernating 70S ribosome, although the interaction is perhaps less stable than in the Mrf-30S complex. Nonetheless, the data unambiguously dissociate hibernation and remodeling of ribosomes, while linking both processes to zinc depletion (Fig. 5E).

#### Mpy-Dependent Ribosome Hibernation and Reduced Drug Sensitivity in Mtb.

To test that Mpy-dependent ribosome hibernation in Mtb is responsive to zinc in a manner similar to *M. smegmatis*, we determined the association of Mpy<sub>Mtb</sub> (Rv3241c) with ribosomes purified from low- and high-zinc cultures of Mtb biofilms. Biofilms cultured in Sauton's medium without supplemental zinc produced an optimum biomass necessary to purify and analyze C– ribosomes (SI Appendix, Fig. S10 A–C). Ribosomes purified from low-zinc biofilms contained higher levels of Mpy<sub>Mtb</sub> than those from high-zinc biofilms, and the increase was dependent on Mrf<sub>Mtb</sub> (Rv0106) (Fig. 6A). We next analyzed the effect of Mpy<sub>Mtb</sub> on degradation of C– ribosomes in growth-arrested Mtb cells using the previously described <sup>3</sup>H-uridine-based assay (12), in which the release of free <sup>3</sup>H-UTP in formic acid extracts of

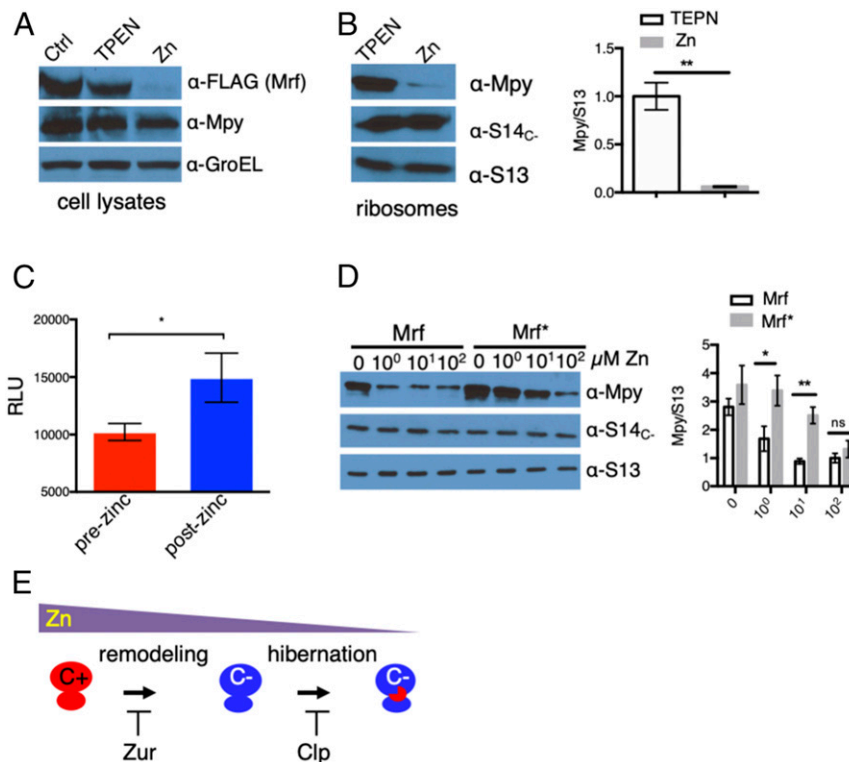


**Fig. 5.** Reactivation of hibernating ribosomes upon zinc replenishment. (A and B) Analysis of Mpy and Mrf in lysates (A) and ribosomes (B) from the YL2 strain after being exposed to zinc following zinc starvation. Cells were cultured in low-zinc Sauton's medium (Ctrl) for 96 h and incubated in low-zinc PBS (TPEN) for 1 h prior to resuspension in high-zinc PBS (Zn) for 1 h. GroEL and ribosomal proteins were probed as controls. The plot shows average Mpy density normalized to S13 from three biologically independent experiments. (C) Activity of 12.5 nM ribosomes purified before or after zinc addition to cultures described in B (mean ± SD from three biologically independent experiments). Activity was measured using nano-luciferase-based in vitro translation assay. (D) Analysis of Mpy in ribosomes from YL2 (Mrf) or YL28 (Mrf\*) strain after exposure to indicated concentrations of zinc for 60 min. Zinc exposure to these cells was done as described in A and B. The plot shows average Mpy density normalized to S13 from four biologically independent experiments. \**P* < 0.05 and \*\**P* < 0.01 (*t* test); ns denotes not significant. (E) A model depicting biphasic adaptation of mycobacteria to zinc depletion, characterized by remodeling and hibernation of ribosomes.

radiolabeled cells was monitored. Zinc-starved wild-type cells harboring hibernating C<sup>-</sup> ribosomes exhibited slower release of <sup>3</sup>H-UTP than those harboring either C<sup>+</sup> or Mpy<sub>Mtb</sub>-free C<sup>-</sup> ribosomes (Fig. 6B). Thus, the global RNA population (a representative measure of ribosomal RNA and, thus, the ribosome) in growth-arrested Mtb cells harboring Mpy-bound ribosomes is more stable than in those with Mpy-free ribosomes. Consistent with the structure-based prediction of reduced Str affinity of Mpy-bound C<sup>-</sup> ribosomes (12), Mtb cells harboring Mpy-bound ribosomes exhibited greater Str tolerance in *in vitro* cultures than cells with either wild-type C<sup>+</sup> or C<sup>-</sup> ribosomes from  $\Delta mpy_{Mtb}$  (Fig. 6C).

The zinc-limiting host environment during chronic infection of Mtb induces the expression of C<sup>-</sup> ribosomes (12), raising the

question as to whether zinc limitation is acute enough to induce Mpy binding to ribosomes. We therefore assessed the effect of Mpy mutation on Mtb growth and drug susceptibility *in vivo*. Because Mpy binding directly reduces the Str sensitivity of ribosomes (12), we reasoned that a change in Str sensitivity of a  $\Delta mpy_{Mtb}$  mutant could be an indirect measure of Mpy<sub>Mtb</sub> activity in Mtb *in vivo*. C3HeB/FeJ mice, which closely mimic human TB pathology and induce the expression of C<sup>-</sup> ribosomes in Mtb (12), were infected with wild-type Mtb (Erdman),  $\Delta mpy_{Mtb}$ , and the complemented strains. Infections were established for 6 wk, followed by 4 and 8 wk of Str treatments. Six weeks of infection was chosen because our previous work found that a majority of Mtb cells expressed C<sup>-</sup> ribosomes by this stage (12). The overall bacterial burden from an untreated  $\Delta mpy_{Mtb}$  infection was

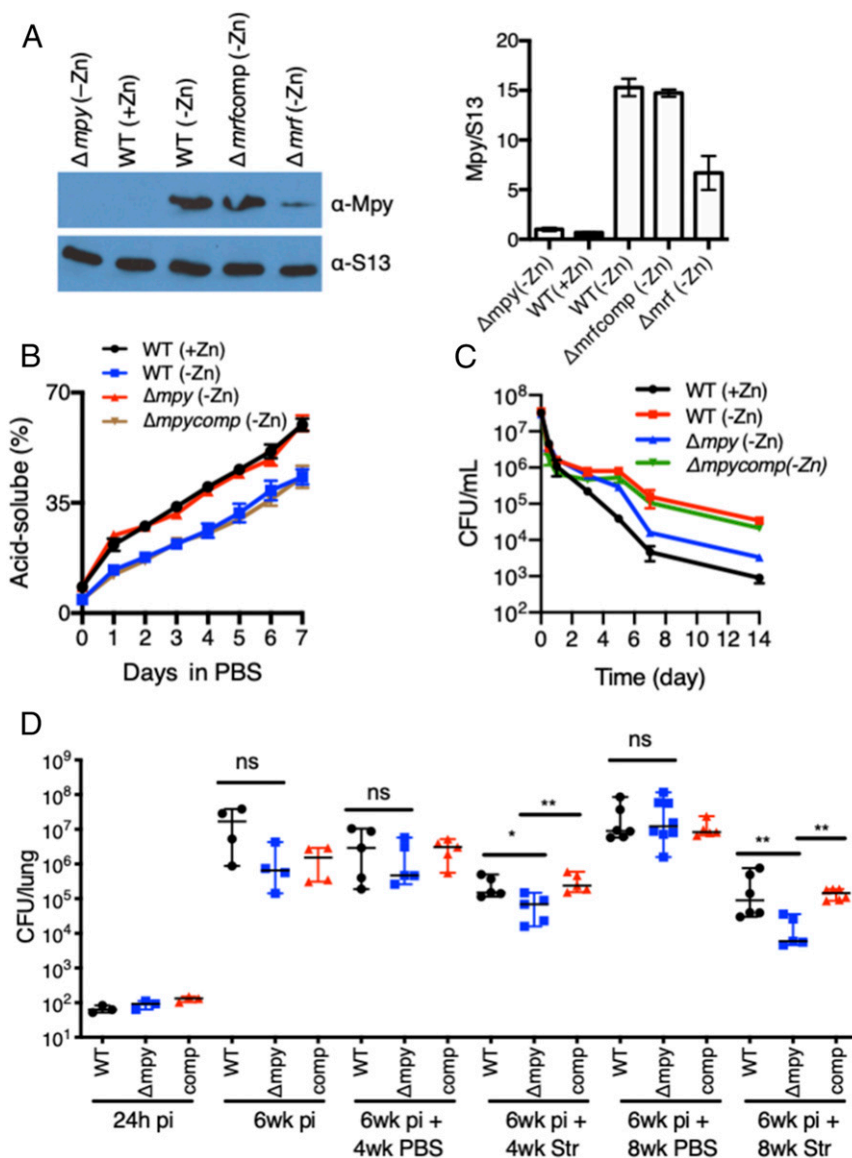


**Fig. 6.** Mpy-dependent Str sensitivity in Mtb *in vitro* and *in vivo*. (A) Growth of Mtb under zinc starvation induces Mrf-dependent Mpy binding to the ribosome. Ribosomes (2.4 pmoles) from pellicles of wild-type (WT) Mtb (*mc*<sup>2</sup>7000) or indicated isogenic mutants, cultured in Sauton's medium with either 1 mM ZnSO<sub>4</sub> (+Zn) or no zinc supplement (-Zn) for 7 wk, were probed with antibodies against *M. smegmatis* Mpy. The plot shows average Mpy density normalized to S13 from two biologically independent experiments. (B) Degradation of ribosomes in the indicated strains of Mtb under growth stasis. Cells from <sup>3</sup>H-uridine (1  $\mu$ Ci/mL)-labeled 7-wk pellicles in +/-Zn medium were resuspended in PBS with tyloxapol (PBSTy), and radioactive counts in formic acid extracts were determined at the indicated time points. (C) *In vitro* Str sensitivity of the indicated Mtb (*mc*<sup>2</sup>7000) strains under growth stasis. Cells from 7-wk pellicles in +/-Zn medium were resuspended in PBSTy containing Str (5  $\mu$ g/mL) and plated at the indicated time points post exposure. Data in A–C represent mean  $\pm$  SD; *n* = 3. (D) Mpy-dependent Str sensitivity of Mtb (Erd) 6 wk post infection (pi) in C3HeB/FeJ mice. Antibiotic and placebo (PBS) were administered for either 4 or 8 wk. Each data point corresponds to one animal. \**P* < 0.05 and \*\**P* < 0.01 (Mann–Whitney *U* test); ns denotes not significant.

similar to wild type, but Str treatment resulted in a ~20-fold greater decline in the bacterial burden of a  $\Delta mpy_{Mtb}$  infection compared to wild type (Fig. 6D). These data suggest that more than 90% of bacilli during chronic infection utilize Mpy<sub>Mtb</sub> at levels that confer measurable resistance to ribosome-targeting antibiotics. However, the number of bacilli with saturating levels of Mpy-bound ribosomes remains indiscernible from these data.

## Discussion

We previously reported that zinc starvation in mycobacteria induces ribosome remodeling, and hibernation of the remodeled ribosome (12). The findings raised the question as to how these processes are coordinated in response to zinc as a specific signal (38, 39). Addressing this question, we show here that ribosome remodeling and hibernation are induced at different levels of zinc. Remodeling is induced when the zinc level drops to ~4 µg/g of biomass, which is growth permissive and supports protein synthesis through the activity of C– ribosomes. However, Mpy binding to the ribosome and subsequent hibernation are promoted when the zinc level drops further by approximately two-fold. Moreover, during the growth phase when C– ribosomes are assembled and remain active, Mpy binding is inhibited by degradation of Mrf, which is transcriptionally coregulated with C– ribosomes. Mrf degradation requires the Clp protease system and that zinc be above a concentration of ~2 µg/g of biomass. This two-tiered transcriptional and posttranslational regulations of Mrf highlights a biphasic adaptation in mycobacteria, in which regulation of *c–* operon by Zur and Clp-Mrf interaction are two distinct molecular checkpoints that probably allow gradual downshift of metabolism in response to limiting zinc (Fig. 5E).

While the findings in this study clearly support Mrf as a target of the Clp protease system, a transient Mrf accumulation during transcription derepression suggests a complex mechanism underlying Mrf-Clp interaction. Moreover, the responsiveness of Mrf accumulation to Zur (SI Appendix, Fig. S3F), and not to the growth phase, suggests that at least one component of the Clp system dedicated to Mrf degradation is Zur regulated. In a preliminary RNA-sequencing experiment we did not observe any significant effect of zinc depletion on the expression of the annotated *clp* genes; perhaps an additional unknown Zur-regulated protein is involved in ClpS-dependent recruitment of Mrf to ClpP1P2 protease. Such a scenario can be compared with the ClpF-ClpS adaptor complex for substrate recruitment to the Clp protease system in *Arabidopsis thaliana* (40). Further complexities in the regulation of Mrf degradation and ribosome hibernation are highlighted by the data that, despite intracellular accumulation of Mrf in YL2 cells at the 24-h stage (Fig. 1C), the Mrf signal in ribosomes was significantly less compared to cells at the 96-h stage (SI Appendix, Fig. S11 A–C). It is tempting to speculate that zinc-bound Mrf synthesized during initial stages of

transcription derepression remains trapped in a ClpS complex, awaiting accumulation of an additional Zur-regulated factor for recruitment to ClpP1P2 protease. Moreover, an earlier-than-normal induction of ribosome hibernation in a *clpS* mutant (Fig. 3E) suggests that zinc binding to Mrf per se may not inhibit its binding to the ribosome; instead, the rate at which Mrf is able to complex with ClpS likely determines its inaccessibility to the ribosomes. Thus, the inability of ClpS to interact with zinc-free Mrf may result in the formation of the Mrf-ribosome complex.

Binding of Mrf to the 30S subunit appears to be an initial step in the process of ribosome hibernation. Mrf could probably sequester the ribosome from translation initiation, inducing conformational changes in the 30S subunit to increase its affinity for Mpy. Moreover, previously proposed kinetic favorability to ribosome-Hpf/pY interactions by growth-rate-dependent down-regulation of translation initiation factors (41, 42) may also be necessary to achieve saturating levels of the Mpy-ribosome complex in a zinc-starved mycobacterial cell. The cell-free recruitment of Mpy without ATP/GTP is consistent with the lack of the signature GTP hydrolysis (G-) domain in Mrf (43), although energy is likely consumed in Clp-dependent Mrf degradation during reactivation of hibernating ribosomes. We note that the reactivation mechanism of hibernating C– ribosomes is very distinct from the recently discovered HflX-dependent reactivation of 100S disomes in *Staphylococcus aureus* (44), underscoring the diverse mechanisms leading to hibernation and reactivation of ribosomes in bacteria. Although zinc-dependent signaling of ribosome hibernation remains to be explored beyond mycobacteria, the process may have evolved from intense competition for free zinc in both environmental and host-pathogen contexts. The Mpy-dependent Str tolerance of Mtb in vivo indeed supports the idea of ribosome hibernation during chronic TB infection. Investigations of Mpy and Mrf contributions to long-term survival of Mtb in hosts may lead to a shorter TB regimen.

## Materials and Methods

Referenced details of routine genetic manipulation of mycobacteria, including lists of strains and plasmids (SI Appendix, Table S1) and oligonucleotides (SI Appendix, Table S2) along with biochemical experiments, are provided as SI Appendix.

**Data Availability.** All relevant data of this study and methods used are presented within the paper and SI Appendix.

**ACKNOWLEDGMENTS.** This work was supported by NIH Grants AI132422 and AI144474 (to A.K.O.). We also acknowledge support from the Wadsworth Center core facilities—The Advanced Light Microscopy and Image Analysis and Applied Genomic Technologies. We thank Patricia Lederman, Kayla Mehigan, and Patrick Kerin for technical assistance; Dr. Patrick Parsons for advice on ICP-MS; Drs. Keith Derbyshire, Todd Gray, Graham Hatfull, and William Jacobs Jr. for gifts of plasmids; and Dr. Keith Derbyshire for critical reading of the manuscript.

1. J. Furin, H. Cox, M. Pai, Tuberculosis. *Lancet* **393**, 1642–1656 (2019).
2. S. Ehrh, D. Schnappinger, K. Y. Rhee, Metabolic principles of persistence and pathogenicity in *Mycobacterium tuberculosis*. *Nat. Rev. Microbiol.* **16**, 496–507 (2018).
3. A. Wada, Y. Yamazaki, N. Fujita, A. Ishihama, Structure and probable genetic location of a “ribosome modulation factor” associated with 100S ribosomes in stationary-phase *Escherichia coli* cells. *Proc. Natl. Acad. Sci. U.S.A.* **87**, 2657–2661 (1990).
4. Y. Maki, H. Yoshida, A. Wada, Two proteins, YfiA and YhbH, associated with resting ribosomes in stationary phase *Escherichia coli*. *Genes Cells* **5**, 965–974 (2000).
5. M. Ueta, C. Wada, A. Wada, Formation of 100S ribosomes in *Staphylococcus aureus* by the hibernation promoting factor homolog SaHPF. *Genes Cells* **15**, 43–58 (2010).
6. M. Ueta et al., Conservation of two distinct types of 100S ribosome in bacteria. *Genes Cells* **18**, 554–574 (2013).
7. M. Ueta et al., Ribosome binding proteins YhbH and YfiA have opposite functions during 100S formation in the stationary phase of *Escherichia coli*. *Genes Cells* **10**, 1103–1112 (2005).
8. Y. S. Polikanov, G. M. Blaha, T. A. Steitz, How hibernation factors RMF, HPF, and YfiA turn off protein synthesis. *Science* **336**, 915–918 (2012).
9. L. E. Franken et al., A general mechanism of ribosome dimerization revealed by single-particle cryo-electron microscopy. *Nat. Commun.* **8**, 722 (2017).
10. B. Beckert et al., Structure of the *Bacillus subtilis* hibernating 100S ribosome reveals the basis for 70S dimerization. *EMBO J.* **36**, 2061–2072 (2017).
11. I. Khusainov et al., Structures and dynamics of hibernating ribosomes from *Staphylococcus aureus* mediated by intermolecular interactions of HPF. *EMBO J.* **36**, 2073–2087 (2017).
12. Y. Li et al., Zinc depletion induces ribosome hibernation in mycobacteria. *Proc. Natl. Acad. Sci. U.S.A.* **115**, 8191–8196 (2018).
13. D. Matzov et al., The cryo-EM structure of hibernating 100S ribosome dimer from pathogenic *Staphylococcus aureus*. *Nat. Commun.* **8**, 723 (2017).
14. D. E. Agafonov, V. A. Kolb, I. V. Nazimov, A. S. Spirin, A protein residing at the subunit interface of the bacterial ribosome. *Proc. Natl. Acad. Sci. U.S.A.* **96**, 12345–12349 (1999).
15. R. K. Flygaard, N. Boegholm, M. Yusupov, L. B. Jenner, Cryo-EM structure of the hibernating *Thermus thermophilus* 100S ribosome reveals a protein-mediated dimerization mechanism. *Nat. Commun.* **9**, 4179 (2018).
16. A. Basu, M. N. Yap, Ribosome hibernation factor promotes *Staphylococcal* survival and differentially represses translation. *Nucleic Acids Res.* **44**, 4881–4893 (2016).
17. B. C. Kline, S. L. McKay, W. W. Tang, D. A. Portnoy, The *Listeria monocytogenes* hibernation-promoting factor is required for the formation of 100S ribosomes, optimal fitness, and pathogenesis. *J. Bacteriol.* **197**, 581–591 (2015).

18. G. Akanuma *et al.*, Ribosome dimerization is essential for the efficient regrowth of *Bacillus subtilis*. *Microbiology* **162**, 448–458 (2016).
19. S. L. McKay, D. A. Portnoy, Ribosome hibernation facilitates tolerance of stationary-phase bacteria to aminoglycosides. *Antimicrob. Agents Chemother.* **59**, 6992–6999 (2015).
20. T. Akiyama *et al.*, Resuscitation of *Pseudomonas aeruginosa* from dormancy requires hibernation promoting factor (PA4463) for ribosome preservation. *Proc. Natl. Acad. Sci. U.S.A.* **114**, 3204–3209 (2017).
21. T. Prossliner, K. Skovbo Winther, M. A. Sørensen, K. Gerdes, Ribosome hibernation. *Annu. Rev. Genet.* **52**, 321–348 (2018).
22. K. Izutsu, A. Wada, C. Wada, Expression of ribosome modulation factor (RMF) in *Escherichia coli* requires ppGpp. *Genes Cells* **6**, 665–676 (2001).
23. K. Tagami *et al.*, Expression of a small (p)ppGpp synthetase, YwaC, in the (p)ppGpp(0) mutant of *Bacillus subtilis* triggers YvyD-dependent dimerization of ribosome. *MicrobiologyOpen* **1**, 115–134 (2012).
24. K. S. Williamson *et al.*, Heterogeneity in *Pseudomonas aeruginosa* biofilms includes expression of ribosome hibernation factors in the antibiotic-tolerant subpopulation and hypoxia-induced stress response in the metabolically active population. *J. Bacteriol.* **194**, 2062–2073 (2012).
25. A. Basu, K. E. Shields, C. S. Eickhoff, D. F. Hoft, M. N. Yap, Thermal and nutritional regulation of ribosome hibernation in *Staphylococcus aureus*. *J. Bacteriol.* **200**, e00426-18 (2018).
26. S. Priscic *et al.*, Zinc regulates a switch between primary and alternative S18 ribosomal proteins in *Mycobacterium tuberculosis*. *Mol. Microbiol.* **97**, 263–280 (2015).
27. K. S. Makarova, V. A. Ponomarev, E. V. Koonin, Two C or not two C: Recurrent disruption of Zn-ribbons, gene duplication, lineage-specific gene loss, and horizontal gene transfer in evolution of bacterial ribosomal proteins. *Genome Biol.* **2**, RESEARCH0033 (2001).
28. A. Dow, S. Priscic, Alternative ribosomal proteins are required for growth and morphogenesis of *Mycobacterium smegmatis* under zinc limiting conditions. *PLoS One* **13**, e0196300 (2018).
29. K. R. Schmitz, D. W. Carney, J. K. Sello, R. T. Sauer, Crystal structure of *Mycobacterium tuberculosis* ClpP1P2 suggests a model for peptidase activation by AAA+ partner binding and substrate delivery. *Proc. Natl. Acad. Sci. U.S.A.* **111**, E4587–E4595 (2014).
30. R. T. Sauer, T. A. Baker, AAA+ proteases: ATP-fueled machines of protein destruction. *Annu. Rev. Biochem.* **80**, 587–612 (2011).
31. A. O. Olivares, T. A. Baker, R. T. Sauer, Mechanistic insights into bacterial AAA+ proteases and protein-remodelling machines. *Nat. Rev. Microbiol.* **14**, 33–44 (2016).
32. J. H. Lo, T. A. Baker, R. T. Sauer, Characterization of the N-terminal repeat domain of *Escherichia coli* ClpA-A class I Clp/HSP100 ATPase. *Protein Sci.* **10**, 551–559 (2001).
33. A. Varshavsky, N-degron and C-degron pathways of protein degradation. *Proc. Natl. Acad. Sci. U.S.A.* **116**, 358–366 (2019).
34. D. A. Dougan, K. N. Truscott, K. Zeth, The bacterial N-end rule pathway: Expect the unexpected. *Mol. Microbiol.* **76**, 545–558 (2010).
35. R. L. Ninnis, S. K. Spall, G. H. Talbo, K. N. Truscott, D. A. Dougan, Modification of PATase by L/F-transferase generates a ClpS-dependent N-end rule substrate in *Escherichia coli*. *EMBO J.* **28**, 1732–1744 (2009).
36. X. Gao, J. Yeom, E. A. Groisman, The expanded specificity and physiological role of a widespread N-degron recognin. *Proc. Natl. Acad. Sci. U.S.A.* **116**, 18629–18637 (2019).
37. J. D. Marsee, A. Ridings, T. Yu, J. M. Miller, *Mycobacterium tuberculosis* ClpC1 N-terminal domain is dispensable for adaptor protein-dependent allosteric regulation. *Int. J. Mol. Sci.* **19**, 3651 (2018).
38. Y. Li *et al.*, Reply to Tobiasson *et al.*: Zinc depletion is a specific signal for induction of ribosome hibernation in mycobacteria. *Proc. Natl. Acad. Sci. U.S.A.* **116**, 2398–2399 (2019).
39. V. Tobiasson, A. Dow, S. Priscic, A. Amunts, Zinc depletion does not necessarily induce ribosome hibernation in mycobacteria. *Proc. Natl. Acad. Sci. U.S.A.* **116**, 2395–2397 (2019).
40. K. Nishimura *et al.*, Discovery of a unique Clp component, ClpF, in chloroplasts: A proposed binary ClpF-ClpS1 adaptor complex functions in substrate recognition and delivery. *Plant Cell* **27**, 2677–2691 (2015).
41. M. R. Sharma *et al.*, PSRP1 is not a ribosomal protein, but a ribosome-binding factor that is recycled by the ribosome-recycling factor (RRF) and elongation factor G (EF-G). *J. Biol. Chem.* **285**, 4006–4014 (2010).
42. H. Yoshida, M. Ueta, Y. Maki, A. Sakai, A. Wada, Activities of *Escherichia coli* ribosomes in IF3 and RMF change to prepare 100S ribosome formation on entering the stationary growth phase. *Genes Cells* **14**, 271–280 (2009).
43. C. E. Haas *et al.*, A subset of the diverse COG0523 family of putative metal chaperones is linked to zinc homeostasis in all kingdoms of life. *BMC Genomics* **10**, 470 (2009).
44. A. Basu, M. N. Yap, Disassembly of the *Staphylococcus aureus* hibernating 100S ribosome by an evolutionarily conserved GTPase. *Proc. Natl. Acad. Sci. U.S.A.* **114**, E8165–E8173 (2017).